JOURNAL OF PROPULSION AND POWER
Vol. 21, No. 2, March–April 2005

Technical Notes

TECHNICAL NOTES are short manuscripts describing new developments or important results of a preliminary nature. These Notes cannot exceed 6 manuscript pages and 3 figures; a page of text may be substituted for a figure and vice versa. After informal review by the editors, they may be published within a few months of the date of receipt. Style requirements are the same as for regular contributions (see inside back cover).

Numerical Study of the Starting Process in a Supersonic Nozzle

A.-S. Mouronval* and A. Hadjadj†
Institut National des Sciences Appliquées, Complexe de Recherche Interprofessionnel en Aerothermochimie, 76801 Saint-Etienne du Rouvray, France

Introduction

DURING the start-up and shut-down transients of rocket nozzles, the overexpanded character of the exhaust jet may lead to complex flow evolutions. In a few milliseconds, multiple shock waves and contact discontinuities with increasing intensities occur and act on the internal nozzle walls. Consequently, the pressure distribution may deviate from its usual symmetric shape, producing significant asymmetric forces (called side loads). Theses loads are prejudicial to the mechanical structure of the nozzle and can cause damage. Therefore, their correct prediction is required when designing nozzles. Nevertheless, the mechanisms of shock wave propagation and related side-loads generation during nozzle start-up are quite complex, and fundamental knowledge of the flow physics is still needed especially during early stages of the starting process.

Transient nozzle flow that exists during engine start-up has been investigated by only a few people. Some experimental work has been performed by Smith,[1] Amann,[2] and Saito et al.[3] Amann,[2] for instance, studied the influence of several parameters (nozzle half-angle, throat width, and nozzle inlet radius) on the starting process in supersonic nozzles driven by a shock tube. Special interest has been paid to the duration of the starting process because it decreases the useful testing time of short-duration facilities. However, the evolution of a complex wave structure has also been shown.

From a numerical point of view, some studies were undertaken to simulate nozzle flow transients. Most of the simulations performed were in the two-dimensional plane or axisymmetric because of the large amount of computational time required for three-dimensional simulations. Prodromou and Hillier,[4] and Igra et al.,[5] for example, carried out Euler simulations of the two-dimensional plane reflection nozzle using a second-order total variation diminishing (TVD) scheme. Jacobs,[6] Tokarcik-Polsky and Cambier and Saito et al.[3] presented numerical simulations of the same type of nozzle, including viscous effects. It may be concluded from these studies that inviscid computations satisfactorily predict the main flow features (namely, the primary and secondary shock waves, multiple shock wave reflections, and slip surfaces). For rocket nozzles, Chen et al.[8] examined the flow structures of the start-up and shut-down processes using a Navier–Stokes solver. The configuration they studied was a subscale nozzle of a J-2S rocket engine, (that is, a precursor of the U.S. space shuttle main engine). Later, Nasuti and Onofri[9] simulated the flow transients during the start-up of the Vulcain nozzle (designed for the European rocket Ariane V). Both inviscid and viscous laminar flow models were considered, which permitted the demonstration that very peculiar flowfield configurations, which are characterized by two main vortical regions, may occur during the start-up of the nozzle. The first region is due to the boundary-layer separation from the wall, whereas the second has an inviscid origin.

The purpose of the present Note is to provide an overview of the phenomena involved in transient nozzle flows (especially at early stages of the start-up) using a weighted essentially nonoscillatory (WENO) scheme, along with a main objective to construct reliable models and accurate prediction tools of side loads.

In a recent work, Mouronval et al.[10] studied numerically the early transient flow induced in an expanding nozzle by an inflow preceded by an incident planar shock wave using high-order numerical methods. Special attention has been paid to the early phase of the starting process and to the appearance of a strong secondary shock wave. A detailed analysis of the wave structure was given, and the mechanism of the formation of vortices on the contact surface has been clearly shown as a result of the high accuracy of the simulations.

The present work is the continuation of the previous one by performing a complete study of Amann's configuration[2] that includes comparisons between numerical results and experimental data.

The test case considered in this study consists of a constant-area tube terminated by a 15-deg plane nozzle whose inlet is rounded, $R = 10$ mm. This nozzle is located at the end wall of a shock tube as shown in Fig. 1.

In the current study, spatial accuracy is achieved by solving the two-dimensional time-dependent Euler equations in a finite-difference form. The fifth-order WENO scheme[11] with adaptive stencils is used to avoid the interpolation across discontinuities and to preserve uniformly high-order approximations at all points where the solution is smooth. Fluxes at cell interfaces are approximated by the Lax–Friedrichs splitting method. The solution is advanced

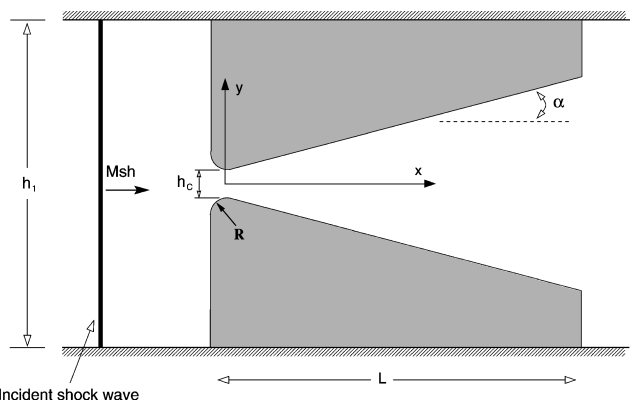

Fig. 1 Configuration: nozzle length $L = 120$ mm, half-nozzle angle $\alpha = 15$ deg, throat height $h_c = 6.15$ mm, shock tube height $h_1 = 104.5$ mm, inlet radius $R = 10$ mm, Mach number of the incident shock wave $M_{sh} = 3$.

Received 29 October 2003; revision received 21 September 2004; accepted for publication 21 September 2004.

*Research Scientist, Laboratoire de Mécanique des Fluides Numérique, Unité Mixte de Recherche 6614, Centre National de la Recherche Scientifique, Avenue de l'Université, Rouen.

†Senior Research Scientist, Laboratoire de Mécanique des Fluides Numérique, Unité Mixte de Recherche 6614, Centre National de la Recherche Scientifique, Avenue de l'Université, Rouen.

in time via the explicit third-order Runge–Kutta TVD method of Shu et al.[12] The detailed description of the numerical scheme is out of the scope of this paper and may be found in the original works by Jiang et al.[11] and Liu et al.[13] The Courant–Friedrichs–Lewy number used in all of the computations presented in this paper was set at 0.8. Additionally, this scheme was coded for structured meshes in general curvilinear coordinates, and parallelization was introduced by partitioning the computational domain and using message passing interface libraries. The numerical code used in this study has been tested and validated on complex compressible flows including shock/shock, shock/mixing-layer interactions,[14,15] and turbulence.[16]

Calculations were performed only for the upper-half of the domain due to the symmetry of the configuration. The mesh was made of 24 domains, each one was assigned to a single processor and contained about (100×120) cells.

High-order numerical schemes require a careful implementation of boundary conditions to eliminate the problem of numerical instability at boundaries. Thus, on the inflow plane (shock tube inlet), all variables are prescribed, which is consistent with supersonic inflow ($M = 1.35$ for $M_{sh} = 3$). On the outflow (nozzle exit), the solution is simply calculated by using one-sided high-order extrapolation, and no boundary conditions are imposed. On the symmetry plane, the v component of the velocity is set to zero. On the inviscid wall, the no-penetration boundary condition is treated through the flux. Specifically, when the wall is approached, the scheme is reduced to a third-order WENO scheme to help stabilize the flow and to keep globally the high accuracy of the scheme.

The test flow is air with $\gamma = 1.4$. The incident shock wave propagates at $M_{sh} = 3$ in a medium at rest, whose pressure and temperature are equal to 6.3 kPa and 293 K, respectively.

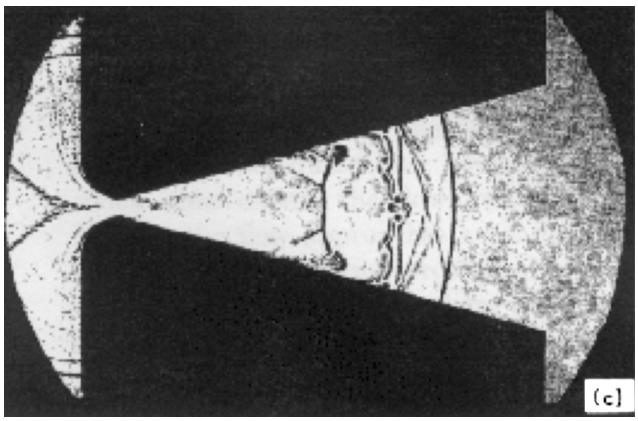

a) Experimental result

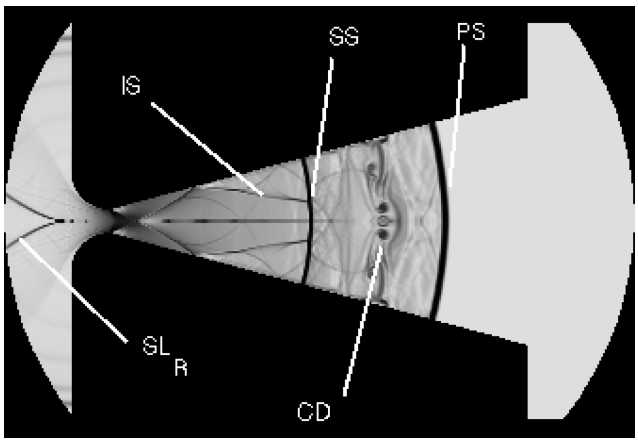

b) Numerical computation

Fig. 2 Schlieren photographs flowfield during start-up at $t^\star \simeq 5.05$.

Results and Discussion

All length scales are normalized by the throat height h_c and the elapsed dimensionless time is defined as $t^\star = t a_0 / h_c$ where a_0 is the speed of sound of the gas initially at rest ($a_0 \simeq 343\ \mathrm{m \cdot s^{-1}}$). The origin of time is chosen in such a way that the primary shock reaches the nozzle throat at $t^\star = 0$.

The general evolution of the wave system within the nozzle is shown in Figs. 2a and 2b. Notice that, basically, the qualitative agreement between numerical and experimental results is rather good. Each feature appearing in the experiment can be easily recognized in the computation.

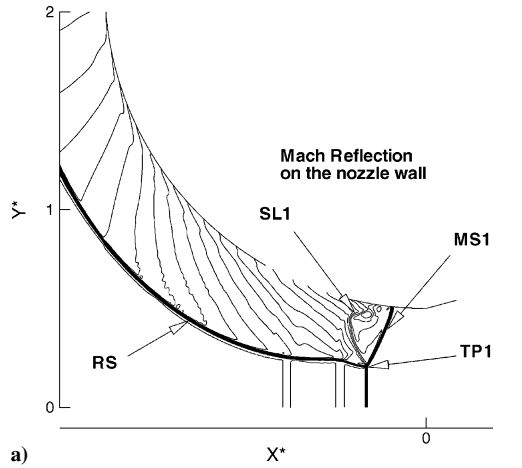

a)

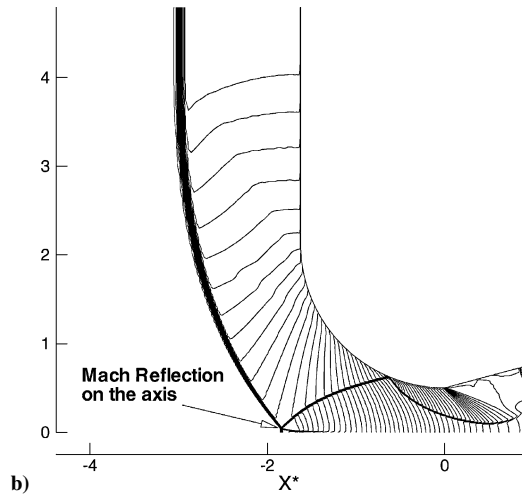

b)

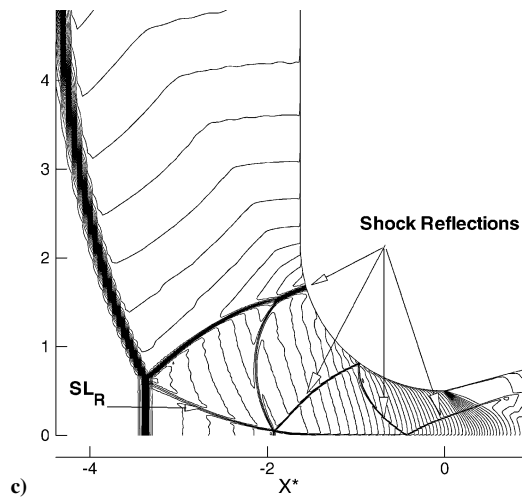

c)

Fig. 3 Density contours; half-plane: a) $t^\star \simeq -8.32e{-}2$, b) $t^\star \simeq 0.59$, and c) $t^\star \simeq 1.70$.

As can be seen (Fig. 2b), when the incident shock reaches the shock tube end wall, its upper and lower parts are reflected and propagate back away from it. They soon collide and create a single reflected shock (RS) leaving behind a quasi-stationary high-pressure region. Meanwhile, the inner core of the incident shock wave is transmitted through the nozzle orifice to form a primary shock (PS) that can be clearly observed propagating in the medium at rest. In addition, when density and pressure fields (not shown) are compared, contact discontinuities (CD) following this primary shock can be easily identified. This discontinuity quickly becomes distorted owing to a Richtmyer–Meshkov type of instability (see Ref. 6). At the same time, a left-running (with respect to the fluid) secondary shock (SS) appears and is carried to the right because of the supersonic carrier flow. This SS arises as a part of the matching process between the high Mach number, low-pressure flow downstream from the throat, and the lower velocity high-pressure gas behind the PS. The flow in the nozzle undergoes an expansion originating from the throat and reflecting several times on the axis. Notice also the appearance of an internal shock (IS) due to a focalization of characteristic lines.

We now discuss in more detail the early stages of this starting process. Special attention will be paid to the flow upstream from the nozzle throat, that is, the region located at $x^\star = x/h_c < 0$, before addressing the flow downstream from it.

As soon as the incident shock reaches the nozzle entrance, its outer part reflects on the wall, whereas its inner part enters the nozzle. The regular reflection occurring on the wall quickly turns into a Mach reflection (Fig. 3a) consisting in the (upper or lower) RS, the PS, that is, transmitted shock, and a Mach stem (MS1). These three shocks meet at a triple point (TP1) where a slip line (SL1) emanates. (See Ben-Dor[17] for more detail about shock wave reflections and associated phenomena in steady and unsteady flows.) As already stated, the two parts of the RS propagate upstream and reflect on the axis (Fig. 3b) via a Mach reflection pattern whose associated slip line SL_R propagates downstream. (A closer look at this SL indicates a Kelvin–Helmholtz instability.) The new part of

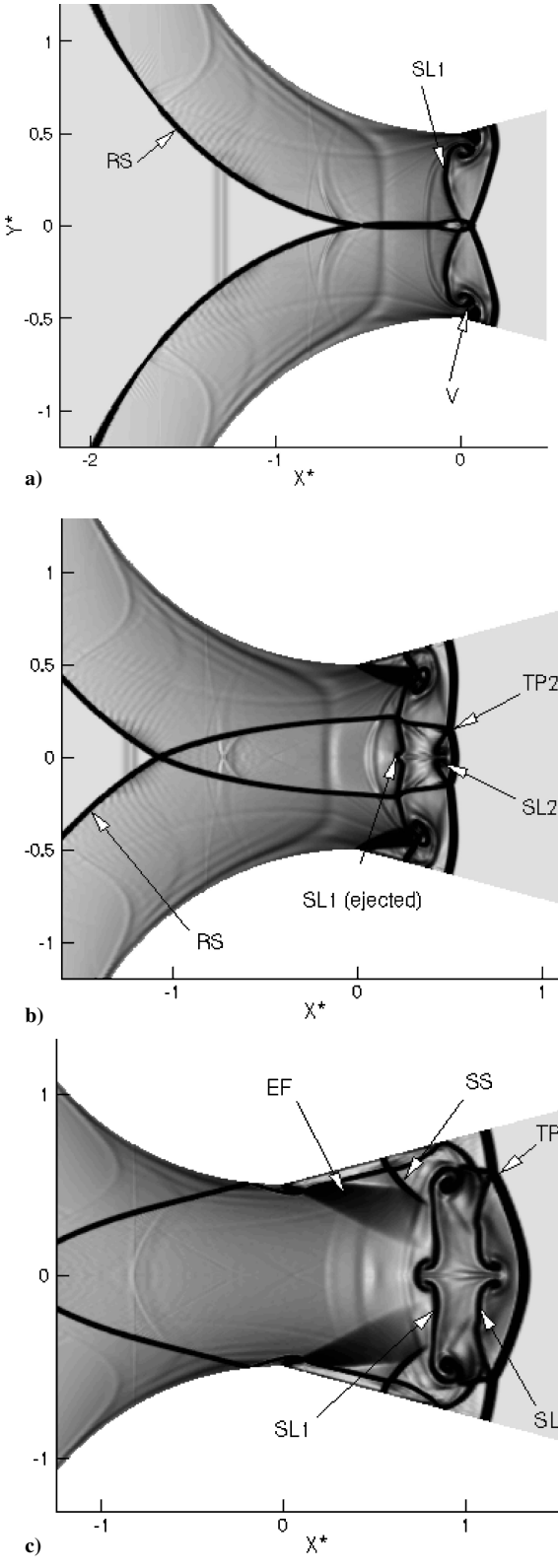

Fig. 4 Numerical schlieren photographs of flowfield during early stages of start-up: a) $t^\star \simeq 2.86e{-}2$, b) $t^\star \simeq 0.14$, and c) $t^\star \simeq 0.36$.

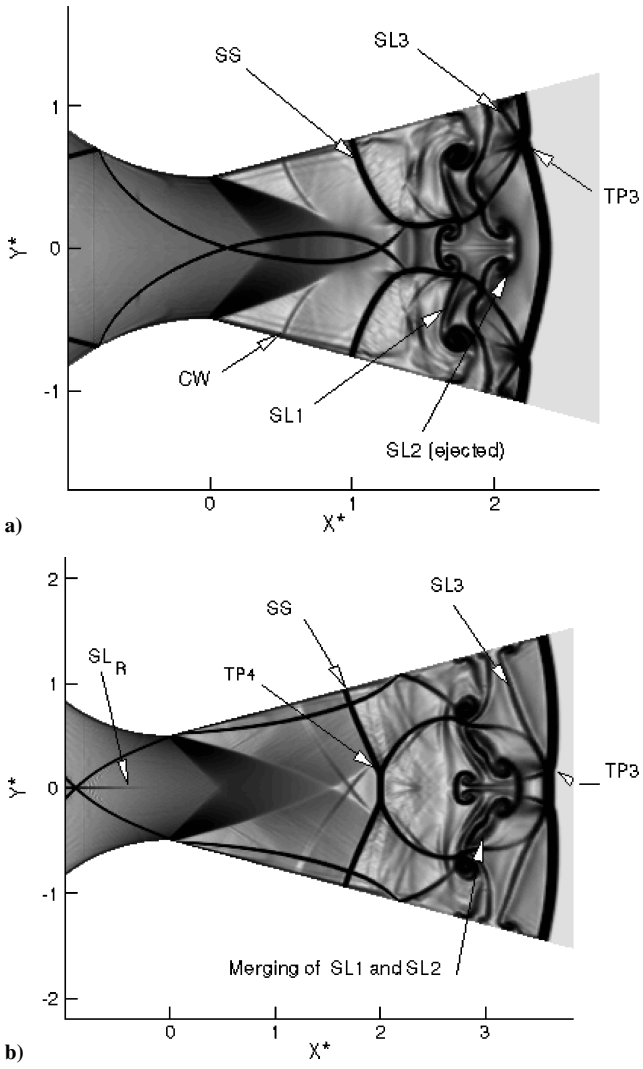

Fig. 5 Numerical schlieren photographs of flowfield during early stages of start-up: a) $t^\star \simeq 0.70$ and b) $t^\star \simeq 1.14$.

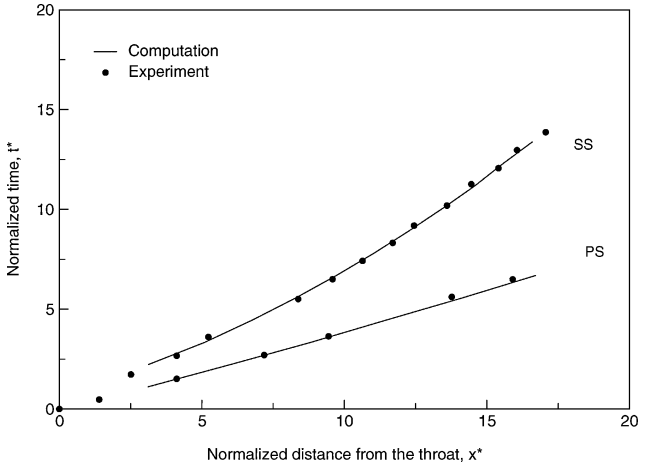

Fig. 6 Comparison of shock waves trajectories on the axis.

this RS reflects on the wall and again on the axis (Fig. 3c) so that additional Mach reflections appear and a multiple wave reflection system is formed. Furthermore, note that the TPs associated with these Mach reflections have a common trajectory, and hence, their SLs match the first one SL_R.

For the flow downstream from the throat, the situation is even more complex. First, the TP1 moves toward the axis and the size of the MS1 grows. As the TP1 disappears (Fig. 4a), its SL is ejected and develops into a vortex V. Again, the regular reflection of MS1 turns into a Mach reflection and the new TP, TP2, travels toward the wall (Figs. 4b and 4c) before vanishing and ejecting its SL. Moreover, investigating this later figure helps in distinguishing the expansion fan (EF) as well as the SS that appears at its tail. As time proceeds (Figs. 5a and 5b), the complex evolution of the flow can be observed, including compression waves (CW), interaction of the secondary wave with parts of the RS, formation of new TPs, TP3 and TP4, moving either toward the wall or the axis and their associated SLs. The merging of SL1 and SL2 can be clearly seen (Fig. 5b). One can also see that the vortices V due to the first Mach reflection are still visible and are carried downstream. At this point, all of the main features of the flow are present (Fig. 2b).

The locations of the PS and SS are in Fig. 6 and compared with the experimental results. The agreement is excellent for the PS, as well as for the SS.

Conclusions

The major properties of the transient flows developing in a supersonic nozzle driven by a shock tube have been investigated using a fifth-order WENO scheme. The main flow features are satisfactorily predicted by computations and are in good agreement with experimental data. More specifically, the complex evolution of the flow has been analyzed: The multiple wave reflection system formed by the reflection of the incident wave has been underlined, as well as the important role played by Mach reflections in the divergent part of the nozzle, which seem to play a prominent role in the generation of side loads in nozzles. We also highlight the mechanism of formation of vortices on the contact surface. In addition, the simulation reveals the existence of various unsteady motions (PS, SS, contact discontinuities), whose properties play an essential role when important choices need to be made to adjust the design of rocket nozzles.

Acknowledgments

This work was supported by the French National Space Agency (CNES) under convention 02/CNES/0435 within the framework of the Aérodynamique des Tuyères et Arrières-Corps program. The authors are grateful to Alexei Kudryavtsev from Institute of Theoretical and Applied Mechanics, Novosibirsk, Russia for helpful discussions and also would like to acknowledge the Centre de Ressources Informatiques de Haute Normandie, Rouen, France, for providing computational resources.

References

[1]Smith, C. E., "The Starting Process in a Hypersonic Nozzle," *Journal of Fluid Mechanics*, Vol. 24, 1966, pp. 625–640.

[2]Amann, H. O., "Experimental Study of the Starting Process in a Reflection Nozzle," *Physics of Fluids Supplement*, Vol. 12, 1967, pp. 150–153.

[3]Saito, T., Timofeev, E. V., Sun, M., and Takayama, K., "Numerical and Experimental Study of 2-D Nozzle Starting Process," *Proceedings of the 22nd International Symposium on Shock Waves*, London, UK, July 1999, Paper No. 4090.

[4]Prodromou, P., and Hillier, R., "Computation of Unsteady Nozzle Flows," *Proceedings of the 18th International Symposium on Shock Waves*, Vol. 2, Sendai, Japan, 1992, pp. 1113–1118.

[5]Igra, O., Wang, L., Falcovitz, J., and Amann, O., "Simulation of the Starting Flow in a Wedge-Like Nozzle," *International Journal of Shock Waves*, Vol. 8, No. 4, 1998, pp. 235–242.

[6]Jacobs, P. A., "Simulation of Transient Flow in a Shock Tunnel and a High Mach Number Nozzle," ICASE Rept. No. 91-60, July 1991.

[7]Tokarcik-Polsky, S., and Cambier, J.-L., "Numerical Study of Transient Flow Phenomena in Shock Tunnels," *AIAA Journal*, Vol. 32, No. 5, 1994, pp. 971–978.

[8]Chen, C.-L., Chakravarthy, S.-L., and Hung, C.-M., "Numerical Investigation of Separated Nozzle Flows," *AIAA Journal*, Vol. 32, No. 9, 1994, pp. 1836–1843.

[9]Nasuti, F., and Onofri, M., "Viscous and Inviscid Vortex Generation During Startup of Rocket Nozzles," *AIAA Journal*, Vol. 36, No. 5, 1998, pp. 809–815.

[10]Mouronval, A.-S., Hadjadj, A., Kudryavtsev, A., and Vandromme, D., "Numerical Investigation of Transient Nozzle Flow," *International Journal of Shock Waves*, Vol. 12, No. 5, 2003, pp. 403–411.

[11]Jiang, G., and Shu, C.-W., "Efficient Implementation of Weighted Essentially Non-oscillatory Schemes," *Journal of Computational Physics*, Vol. 126, No. 1, 1996, pp. 202–228.

[12]Shu, C.-W., and Osher, S., "Efficient Implementation of Essentially Non-oscillatory Shock Capturing Schemes," *Journal of Computational Physics*, Vol. 83, No. 1, 1989, pp. 32–78.

[13]Liu, X. D., Osher, S., and Chan, T., "Weighted Essentially Non Oscillatory Schemes," *Journal of Computational Physics*, Vol. 115, No. 1, 1994, pp. 200–212.

[14]Kudryavtsev, A., and Khotyanovsky, D. V., "A Numerical Method for Simulation of Unsteady Phenomena in High Speed Shear Flows," *Proceedings of the International Conference on Methods of Aerophysical Research ICMAR'98*, Russian Academy of Sciences, Siberian Div., Inst. of Theoretical and Applied Mechanics, Akademgorok, Novosibirsk, Pt. 1, June 1998.

[15]Kudryavtsev, A., and Hadjadj, A., "Visualisation graphique en mécanique des fluides numérique," *Proceedings of the 9th French Conference on Flow Visualisation and Image Processing*, Centre National de la Recherche Scientifique, Vol. 1, Rouen, France, June 2001, pp. 55–62.

[16]Blin, L., Hadjadj, A., and Vervisch, L., "Large Eddy Simulation of Compressible Turbulent Flows," AIAA Paper 99-0787, Jan. 1999.

[17]Ben-Dor, G., Shock Wave Reflection Phenomena, Springer-Verlag, New York, 1991, Chap. 4.